



Contents lists available at ScienceDirect

Bioorganic & Medicinal Chemistry Letters

journal homepage: www.elsevier.com/locate/bmcl4-Connected azabicyclo[5.3.0]decane Smac mimetics-Zn²⁺ chelators as dual action antitumoral agentsLeonardo Manzoni^a, Alessandro Samela^b, Stefano Barbini^b, Silvia Cairati^a, Marta Penconi^{a,c}, Daniela Arosio^{a,c}, Daniele Lecis^d, Pierfausto Seneci^{b,*}^a Istituto di Scienze e Tecnologie Molecolari (ISTM), Consiglio Nazionale delle Ricerche (CNR), Via Golgi 19, I-20133 Milan, Italy^b Dipartimento di Chimica, Università degli Studi di Milano, Via Golgi 19, I-20133 Milan, Italy^c SmartMatLab Centre, Via Golgi 19, I-20133 Milan, Italy^d Dipartimento di Oncologia Sperimentale e Medicina Molecolare, Fondazione IRCCS Istituto Nazionale Tumori, Via Amadeo 42, I-20133 Milan, Italy

ARTICLE INFO

Article history:

Received 24 February 2017

Revised 8 April 2017

Accepted 11 April 2017

Available online xxxx

Keywords:

Dual action compounds

Smac mimetics

Zinc chelation

Apoptosis

Peptidomimetics

ABSTRACT

Putative dual action compounds (DACs **3a–d**) based on azabicyclo[5.3.0]decane (ABD) Smac mimetic scaffolds linked to Zn²⁺-chelating 2,2'-dipicolylamine (DPA) through their 4 position are reported and characterized. Their synthesis, their target affinity (cIAP1 BIR3, Zn²⁺) in cell-free assays, their pro-apoptotic effects, and their cytotoxicity in tumor cells with varying sensitivity to Smac mimetics are described. A limited influence of Zn²⁺ chelation on in vitro activity of DPA-substituted DACs **3a–d** was sometimes perceivable, but did not lead to strong cellular synergistic effects. In particular, the linker connecting DPA with the ABD scaffold seems to influence cellular Zn²⁺-chelation, with longer lipophilic linkers/DAC **3c** being the optimal choice.

© 2017 Published by Elsevier Ltd.

Multiple pathophysiological mechanisms are connected with the development and the progression of cancer.¹ The ability of cancer cells to develop resistance to chemotherapeutics and target-directed therapies² demands for more effective treatments.³ A dual action compound (DAC) should interfere with two validated mechanisms against cancer, and should thus increase efficacy and minimize resistance.⁴

Smac-DIABLO is a mitochondrial protein with multiple pro-apoptotic effects in cancer cells. It binds to inhibitor of apoptosis proteins⁵ (IAPs), frees caspases-3, -7 and -9,⁶ and induces degradation of cellular IAPs (cIAPs).⁷ Zinc ions show anti-apoptotic effects in cancer cells. They prevent the autocatalytic conversion of procaspase-3 to active caspase-3 by interaction with its “safety catch” DDD sequence,⁸ and their chelation causes serine protease-dependent depletion of anti-apoptotic X-linked IAP (XIAP).⁹

Substituted azabicyclo[5.3.0]decane Smac mimetics (ABDs) are potent, cytotoxic Smac mimetics targeted against IAPs.¹⁰ Positions

4 and 10 of their bicyclic core (Fig. 1) can be substituted to increase their IAP affinity, and their drug-like profile.¹¹ We reasoned that zinc depletion by Zn²⁺-chelating DACs built around ABDs should cause synergistic pro-apoptotic effects. We reported¹² 4-amidoalkyl ABDs substituted in position 10 with a Zn²⁺-chelating moiety (i.e., 2,2'-dipicolylamine, DPA in **1**, Fig. 1). A (S)-PheGly linker connected DPA with Smac mimetic ABD scaffolds (i.e., 4-benzamidomethyl Smac mimetic **2**,¹¹ Fig. 1).

10-Connected Smac mimetic- Zn²⁺-chelator DACs showed cell-free potency against IAPs and Zn²⁺-chelating properties. Their cytotoxicity was moderate, and Zn²⁺ chelation-dependent effects in cellular assays were not observed.¹² We then targeted DPA-containing, ABD-based DACs connected through position 4, bearing an IAP affinity-best diphenylmethanamide substitution in position 10 (generic structure **3**, Fig. 2). In particular, we aimed to evaluate the influence of the linker between DPA and ABD scaffolds on cell-free properties, on biological activity and bioavailability in cancer cells.

Our synthetic strategy required access to gram quantities of N³-Boc-protected 4-amino-10-diphenylmethanamido ABD **4** (Scheme 1). We optimized its synthesis from tricyclic butyl ester

* Corresponding author.

E-mail address: pierfausto.seneci@unimi.it (P. Seneci).

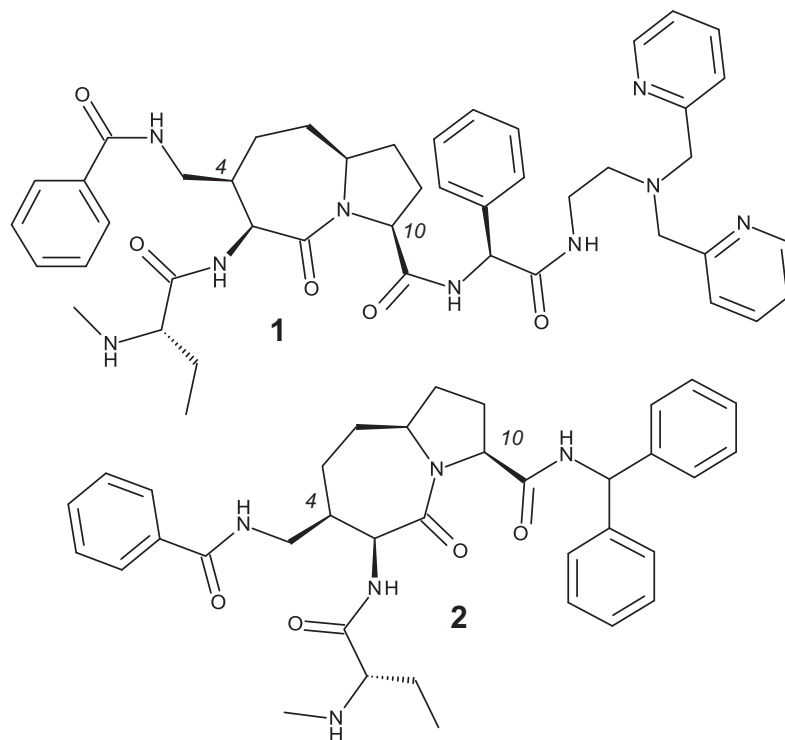


Fig. 1. Structure of ABD-based compounds **1** and **2**.

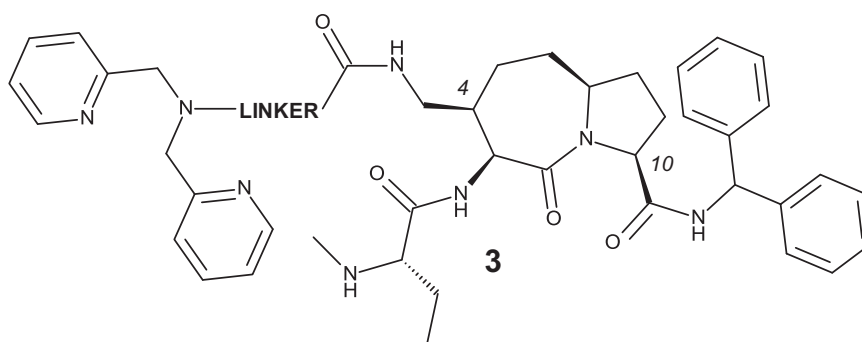


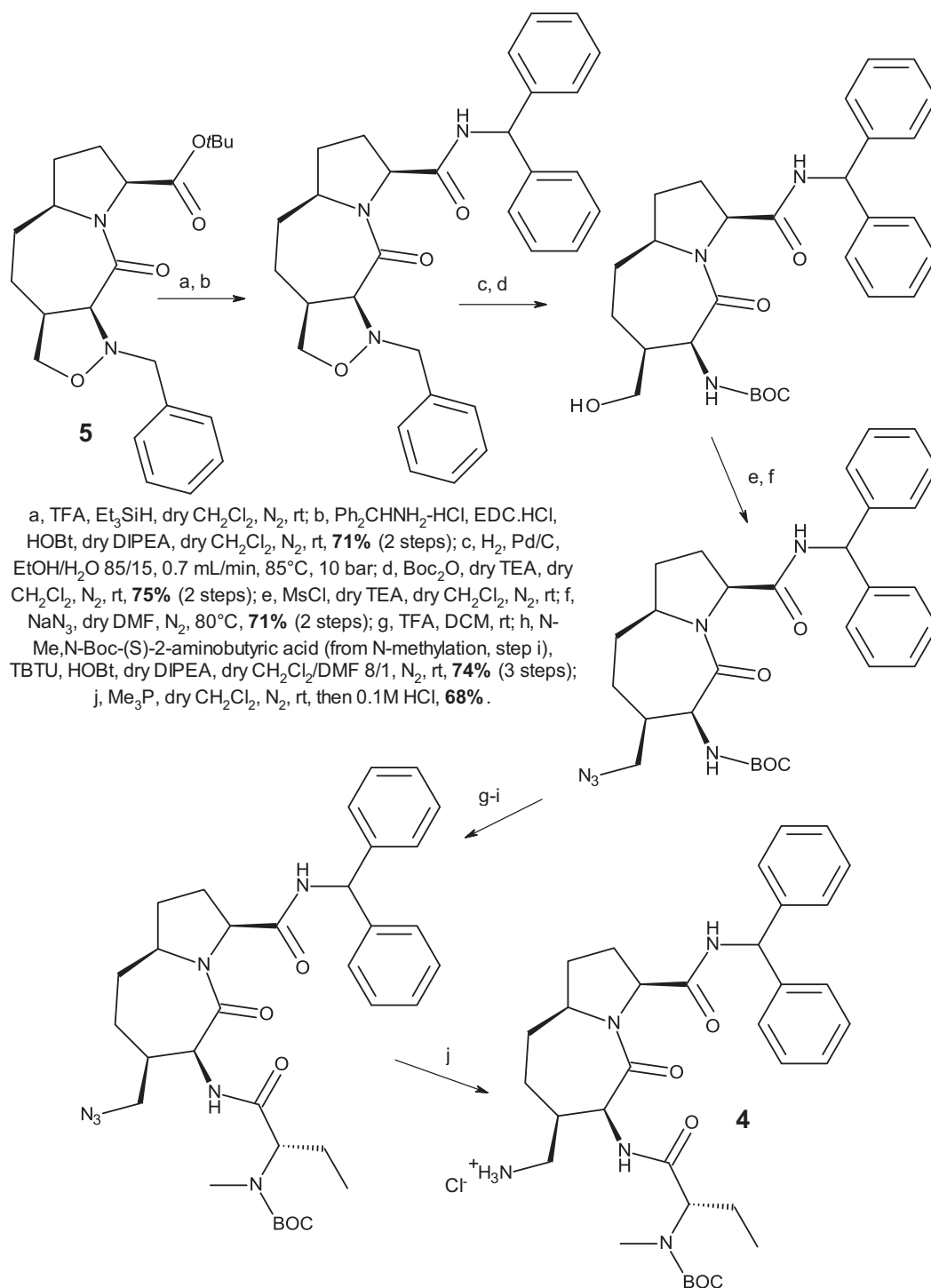
Fig. 2. General structure of 4-connected Smac mimetic- Zn^{2+} -chelator DACs **3**.

5,¹¹ available in large quantity in our lab, by improving yields and simplifying known experimental protocols.¹¹ Scheme 1 shows the 10-step optimized synthesis of amine **4** in an overall $\approx 20\%$ yield from **5**.

We selected *N,N*-bis(2-pyridinylmethyl)glycine **6** as a key DPA-containing synthon (boxed structure, Fig. 3), and we coupled it to key Smac intermediate **4** either as such (compound **3a**, LINKER = CH_2 , “no linker”) or through three linkers with varying length and lipophilicity. Namely, β -alanine (compound **3b**, LINKER = $\text{CH}_2\text{CONH}(\text{CH}_2)_2$, “short lipophilic”), 11-aminoundecanoic acid (compound **3c**, LINKER = $\text{CH}_2\text{CONH}(\text{CH}_2)_{10}$, “long lipophilic”), and 8-amino-3,6-dioxaoctanoic acid (compound **3d**, LINKER = $\text{CH}_2\text{CONH}(\text{CH}_2)_2\text{O}(\text{CH}_2)_2\text{OCH}_2$, “hydrophilic”) were used respectively as short lipophilic, long lipophilic and long hydrophilic linkers (Fig. 3).

DPA-containing synthon **6** was prepared following a published procedure.¹³ Nucleophilic substitution on DPA **7** with ethyl 2-chloroacetate **8** in mild conditions (step a, Scheme 2) led to ester **9**, then hydrolyzed in aqueous KOH and neutralized (step b) to acid **6** in a good, overall $\approx 60\%$ yield. Coupling of carboxylate **6** with amine **4** in basic peptide coupling conditions (step c) led to *N*-Boc-protected **10a**, that was then deprotected in acidic conditions, yielding target “no linker” DAC **3a** (step d, Scheme 2) in a good $\approx 76\%$ yield from **4**.¹⁴

We reasoned that time- and cost-expensive amine **4** should be used as late as possible in a synthetic scheme, to minimize its consumption. Thus, target DACs **3b** and **3c**, where the Zn^{2+} -chelating moiety and the Smac mimetic portion are connected by lipophilic linkers, were prepared by coupling of pre-formed acid DPA-linker constructs **11a,b** with amine **4** (Scheme 3). Commercially available

Scheme 1. Synthesis of key Smac amino ABD intermediate **4**.

β -alanine **12a** and 11-aminoundecanoic acid **12b** were esterified in acid conditions (step a, Scheme 3). Aminoesters **13a**¹⁵ and **13b**¹⁶ were acylated with bromoacetyl bromide in mild basic conditions (step b). Nucleophilic substitution of DPA **7** with bromoesters **14a**¹⁷ and **14b**¹⁶ (step c) led to methyl ester DPA-linker constructs **15a, b**. Aqueous basic hydrolysis (step d) led to target acid DPA-linker constructs **11a, b** with moderate (**11b**, $\approx 21\%$) to good (**11a**, $\approx 44\%$) un-optimized overall yields from aminoacids

12a, b. Coupling of acid DPA-linker constructs **11a, b** with amine **4** in basic peptide coupling conditions (step e) led to *N*-Boc-protected **10b, c**, that were then deprotected in acidic conditions, yielding target DACs **3b, c** (step f, Scheme 3) in a moderate (“long lipophilic” **3c**,¹⁸ $\approx 27\%$) to good (“short lipophilic” **3b**,¹⁴ $\approx 66\%$) un-optimized overall yields from **4**.

The synthesis of DAC **3d**, connected by a hydrophilic linker, took advantage of the commercial availability of *N*-CBz protected

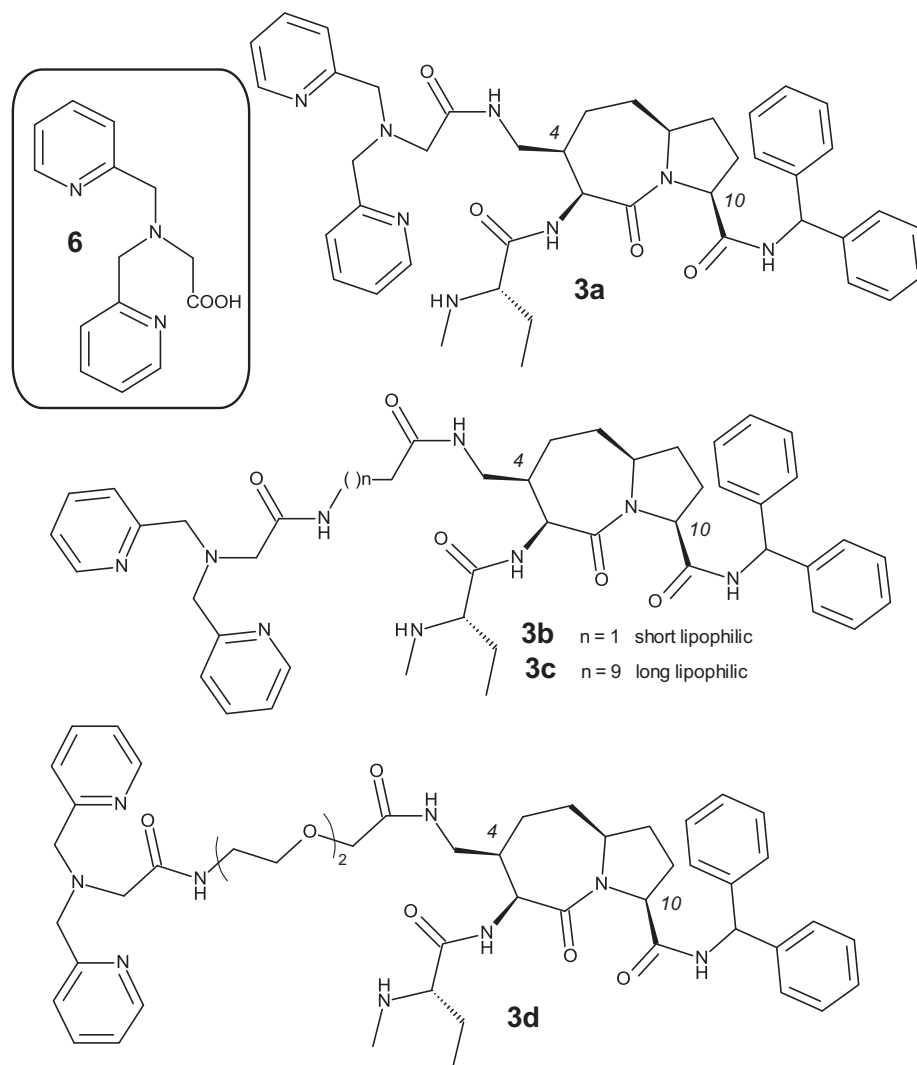


Fig. 3. Structure of DPA-containing synthon **6**, and of 4-connected, ABD-based DACs **3a–d**.

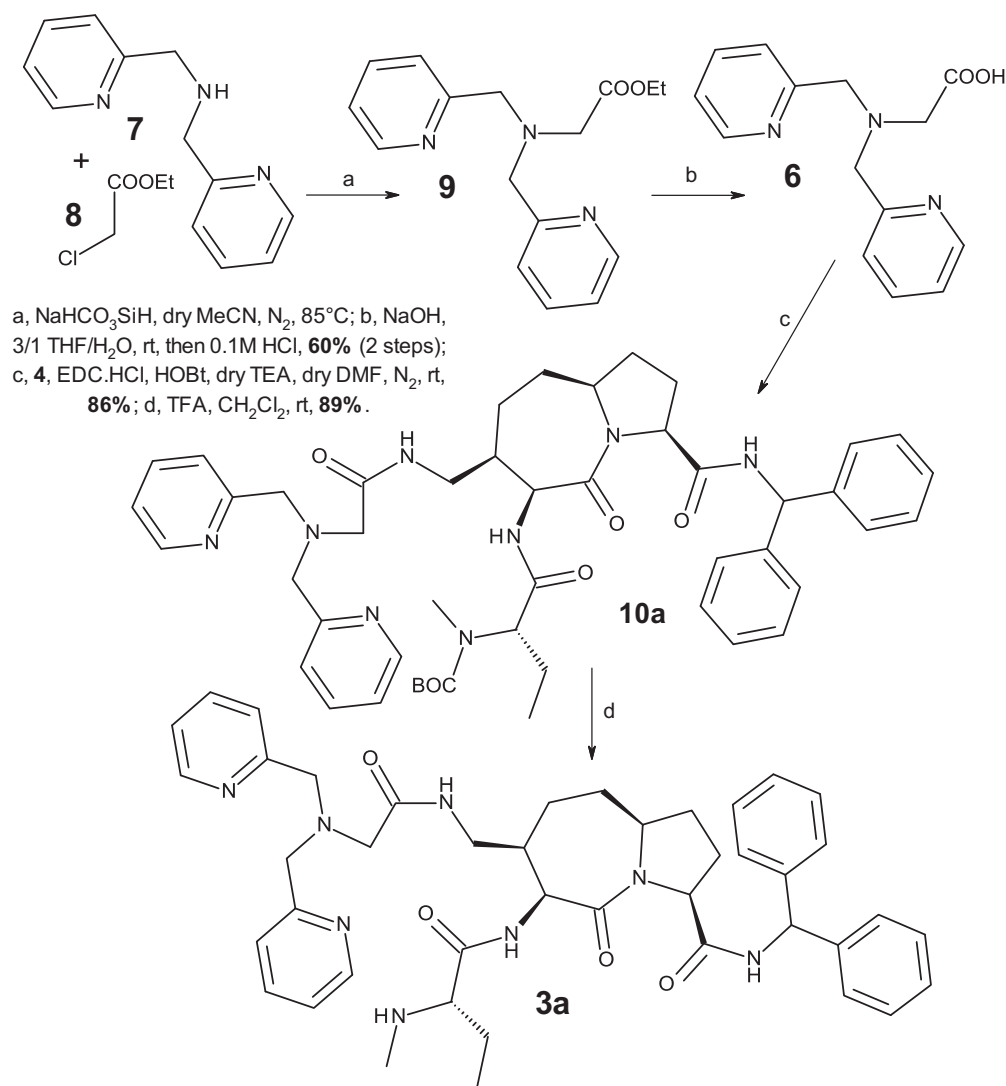
aminoacid **16** (Scheme 4). Its coupling with amine **4** in basic peptide coupling conditions (step a) led to *N*-protected linker-Smac construct **17**. Deprotection of **17** in hydrogenolytic conditions (step b) produced the free amino construct **18**, that was then coupled with the DPA-containing synthon **6** in basic peptide coupling conditions (step c). Acidic deprotection of compound **19** (step d, Scheme 4) yielded target “hydrophilic” DAC **3d** in a moderate, un-optimized $\approx 31\%$ overall yield from **4**.¹⁴

We measured the affinity of 10-connected DAC **1**, of 4-connected DACs **3a–d**, and of standard 4-benzamidomethyl Smac mimetic **2**¹¹ for the BIR3 domain of cIAP1 (Table 1, column 2), using a fluorescence polarization-based assay.¹⁹

The low nM affinity of Smac mimetics such as **2** is maintained either by 10-connected and 4-connected DACs (Table 1). The small decrease in affinity observed for lipophilic **3c** may be due either to a limited hindrance caused by its long lipophilic linker, or to aspecific aggregation of the more lipophilic DAC. Nevertheless, the addition of a Zn^{2+} chelating moiety at either the 10- or the 4-position of ABD-based DACs does not impair their Smac mimetic nature.

We determined the effects of compounds **1**, **3a–d** and **2** on apoptosis-connected cellular processes. Western blots from sensitive (MDA-MB231) and Smac mimetic-resistant breast carcinoma tumor cell lines (MDA-MB453) are respectively shown in Figs. 4 and 5.

Effects on cIAP1 degradation in Smac mimetic-sensitive MDA-MB231 cells are shown on lane 1, Fig. 4. cIAP1 degradation was almost complete for 10-connected DAC **1**, still significant for 4-connected DACs **3a–c** and standard **2**, and lower for 4-connected DAC **3d**, possibly due to limited cell permeability. The activation of apoptosis, quantified through the cleaved forms of caspase-3 (lane 4) and PARP proteins (lane 3), was stronger for 4-connected DACs **3a** and **3c** and standard **2**, still significant for 4-connected DAC **1**, and limited for 4-connected DACs **3b** and **3d**. Cellular pro-apoptotic effects could be influenced by cell permeability and linker length/lipophilicity. The levels of XIAP (lane 2, Fig. 4) should mirror putative Zn^{2+} chelation-mediated effect of DACs on XIAP degradation. Compound **3c** showed significant XIAP degradation, while other compounds did not affect XIAP degradation. We hypothesize that a long lipophilic linker may be needed to exert



Scheme 2. Synthesis of DPA-containing acid **6**, and of 4-connected, ABD-based DAC **3a**.

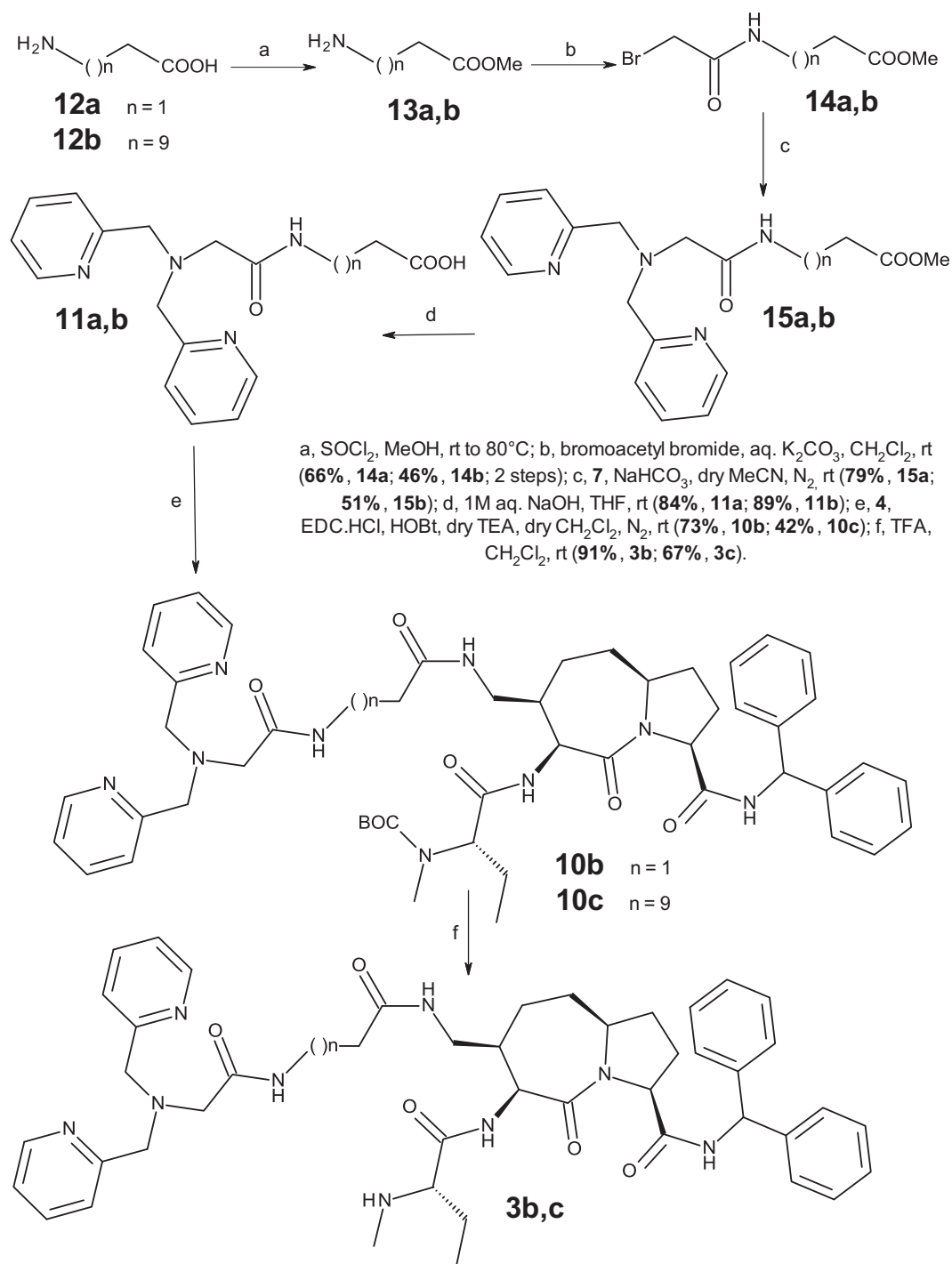
cellular pro-apoptotic Zn^{2+} -chelation, possibly to elongate DPA away from bulky ABD scaffold (no/short linker-containing **3a,b**: inactive).

Effects on Smac mimetic-resistant MDA-MB453 cells (Fig. 5) are weaker, and sometimes different from the ones observed on MDA-MB231 cells. 10-Connected DAC **1** and standard **2** did not show any pro-apoptotic effect in MDA-MB453 cells. 4-Connected DACs **3a–d** caused cIAP1 degradation (lane 1, Fig. 5), but did not activate caspase-3 or PARP (lanes 3 and 4). Lipophilic compound **3c** shows limited XIAP degradation; hydrophilic **3d** shows a slightly higher XIAP degradation (lane 2). The pro-apoptotic activity on MDA-MB453 of **3d** vs. its inactivity on MDA-MB231 cells may be the result of different permeability-availability for hydrophilic compounds in the two cell lines.

We then determined the cytotoxicity of compounds **1**, **2** and **3a–d** on the same cell lines (lanes 3 and 4, Table 1) after 24 h exposure. The inhibition curves of compounds **1**, **3a–d** and **2** on MDA-MB231 cells are shown in Fig. S1, Supporting Information.

Good cytotoxicity ($\leq 5 \mu\text{M}$) could not be observed with 10-connected DACs¹² such as **1** on Smac mimetic-sensitive MDA-MB231 cells. Conversely, in agreement with pro-apoptotic effects shown in Fig. 4, compounds **3a** and in particular **3c** showed good cytotoxicity. As to the latter, we suggest better cell permeability and better Zn^{2+} accessibility for the DPA moiety due to the long lipophilic linker as reasons for its sub-micromolar cytotoxicity on MDA-MB231 cells. Unfortunately, none among tested DACs showed cytotoxicity against MDA-MB453 cells. We suggest that observed effects on cIAP1 and XIAP degradation by DACs **3a**, **3c** and **3d** are not strong enough to induce significant cytotoxicity on Smac-resistant MDA-MB453 cells.

We examined the Zn^{2+} chelating ability of DACs **3a–d**, and of DPA **7** by fluorescence spectroscopy. Changes in their emission spectra in presence of increasing amounts of Zn^{2+} were measured by excitation at 273 nm (**3a–d**) or at 270 nm (**7**), using a published protocol.¹² The fluorescence titration of **3c** is shown in Fig. 6,



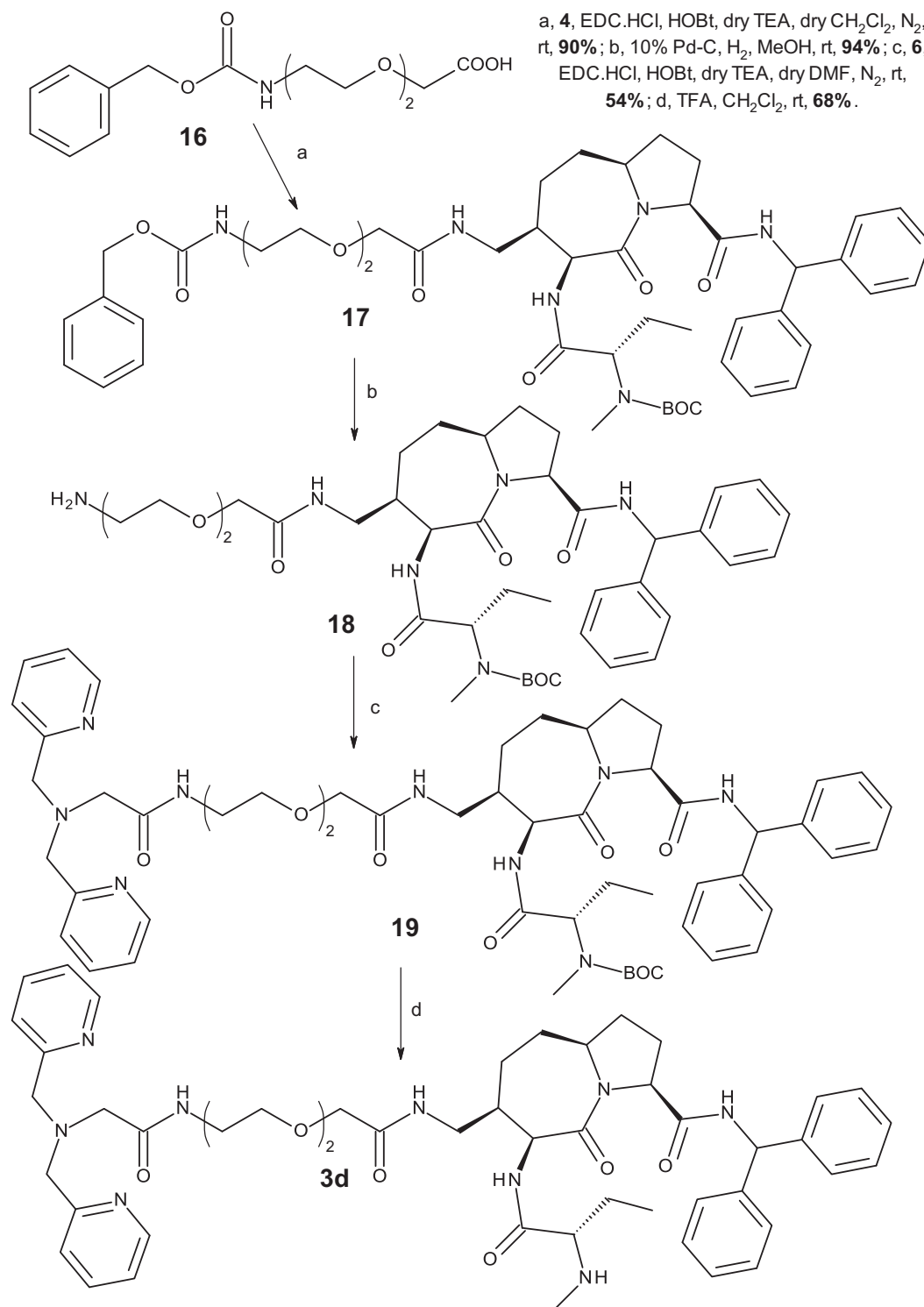
Scheme 3. Synthesis of acid DPA-linker constructs **11a, b**, and of lipophilic 4-connected, ABD-based DACs **3b, c**.

while the others are shown in Figs. S2–S5, Supporting Information.

4-Connected DACs **3a–d** chelate zinc ions similarly to 10-connected DACs,¹² likely through the DPA moiety. A 1:1 Zn^{2+} -DAC stoichiometry was observed for each compound. Thus, the differences observed among compounds **3a–d** in terms of Zn^{2+} chelation-dependent biological effects (degradation of XIAP,

lane 2, Figs. 4 and 5) might be ascribed to *in cellulo* availability of their DPA moiety.

In conclusion, we attached DPA onto the ABD scaffold through a 4-methylamido substituent, using linkers with varying length and lipophilicity. Pro-apoptotic DACs **3a–d** act as Smac mimetics, and show limited, cell-dependent synergistic effects in cellular assays (lipophilic **3c** in MDA-MB231 cells, hydrophilic **3d** in MDA-



Scheme 4. Synthesis of hydrophilic target 4-connected, ABD-based DAC **3d**.

Table 1

clAP1 binding (cell free), cytotoxicity on MDA-MB231 and MDA-MB453 cells.

Compound	clAP1, IC ₅₀ ^a	MDA-MB231, IC ₅₀ ^b	MDA-MB453, IC ₅₀ ^b
1 ¹²	1.09	14.9	>25
2	1.42	4.1	>25
3a	1.52	6.5	>25
3b	1.35	>25	>25
3c	6.08	0.97	>25
3d	1.66	>25	>25

^a nanomolar affinity.

^b IC₅₀, micromolar, measured by CellTiter-Glo (Promega).

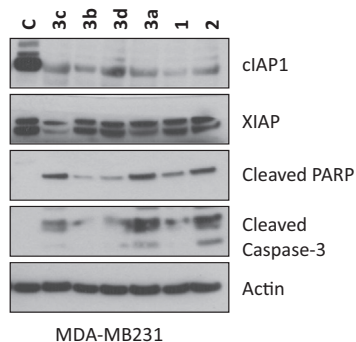


Fig. 4. Pro-apoptotic effects of compounds **1**, **3a–d** and **2** (5 μ M) on Smac mimetic-sensitive MDA-MB231 cells. C, control.

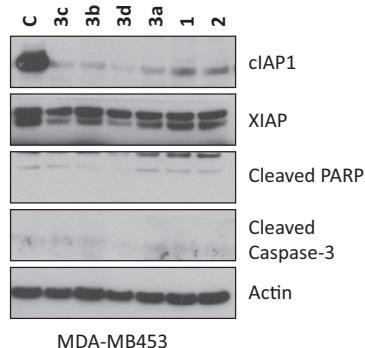


Fig. 5. Pro-apoptotic effects of compounds **1**, **3a–d** and **2** (5 μ M) on Smac mimetic-resistant MDA-MB453 cells. C, control.

MDA453 cells). In particular, compound **3c** is the first ABD-based, DPA-containing DAC reaching sub-micromolar cytotoxicity on MDA-MB231 cells.

We will continue our investigation on Smac mimetic – Zn^{2+} chelator DACs by further studying the cellular effects possibly attributable to Zn^{2+} chelation by compounds **3c,d**; and by studying the influence of other Zn^{2+} chelating moieties on cytotoxic potency and cellular permeation of novel Smac mimetic- Zn^{2+} -chelator DACs. Results will be reported in due time.

Acknowledgments

We gratefully acknowledge MIUR (Ministero dell'Università e della Ricerca) for financial support (PRIN project 2015WW5EH: Tumor-targeting peptidomimetics: synthesis and biomedical applications). The use of instrumentation purchased through the Regione Lombardia – Fondazione Cariplo joint project “SmartMatLab Centre” (decreti 12689/13, 7959/13; Azione 1 e 2) is gratefully acknowledged. M.P. thanks Dr. Alberto Bossi for the discussions on Zn^{2+} chelating experiments.

A. Supplementary data

Supplementary data (Experimental procedures for the synthesis of compounds **4**, **6**, **3a**, **3b**, **3d**. LC–MS and NMR characterization of intermediates and compounds **4**, **6**, **3a–d**. Experimental procedures for cell-free testing/binding affinity determination of DACs and standards in presence of BIR3 constructs from cIAP1. Experimental procedures and Figures for Zn^{2+} titration of compounds **7**, **3a–d**. Experimental procedures and Figures for mechanism of action studies and cellular cytotoxicity testing of DACs and standards against human tumor cell lines) associated with this article can be found, in the online version, at <http://dx.doi.org/10.1016/j.bmcl.2017.04.032>.

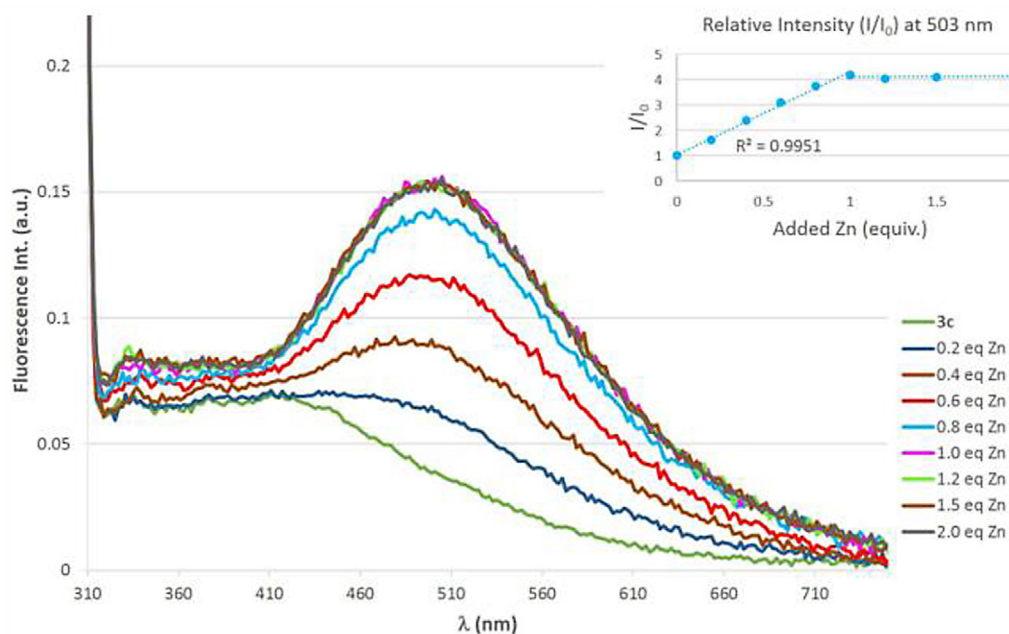


Fig. 6. Fluorescence titration of “long lipophilic” DAC **3c** with increasing $[\text{Zn}^{2+}]$.

References

- Hanahan D, Weinberg RA. *Cell*. 2011;144:646.
- Housman G, Bayler S, Heerboth S, et al. *Cancers*. 2014;6:1769.
- Holohan C, Van Schaeybroeck S, Longley DB, Johnston PG. *Nat Rev Cancer*. 2013;13:714.
- O'Boyle NM, Meegan MJ. *Curr Med Chem*. 2011;18:4722.
- Varfolomeev E, Vucic D. *Future Oncol*. 2011;7:633.
- Mastrangelo E, Cossu F, Milani M, et al. *J Mol Biol*. 2008;384:673.
- Varfolomeev E, Blankenship JW, Wayson SM, et al. *Cell*. 2007;131:669.
- Truong-Tran AQ, Grosser D, Ruffin RE, Murgia C, Zalewski PD. *Biochem Pharmacol*. 2003;66:1459.
- Makhov P, Golovine K, Uzzo RG, et al. *Cell Death Differ*. 2008;15:1745.
- Sun H, Nikolovska-Coleska Z, Yang C-Y, et al. *Acc Chem Res*. 2008;41:1264.
- Seneci P, Bianchi A, Battaglia C, et al. *Bioorg Med Chem*. 2009;17:5834.
- Manzoni L, Gornati D, Manzotti M, et al. *Bioorg Med Chem Lett*. 2016;26:4613.
- Åstrand OAH, Aziz G, Farzand Ali S, Paulsen RE, Vidar Hansen T, Rongved P. *Bioorg Med Chem*. 2013;21:5175.
- The experimental protocol to intermediates 4 and 6, and to 4-connected DACs **3a**, **3b** and **3d**, and their analytical characterization are reported in the Supplementary Information.
- Dekker FJ, Ghizzoni M, van der Meer N, Wisastra G, Haisma HJ. *Bioorg Med Chem*. 2009;17:460.
- Minazzi P, Lattuada L, Menegotto IG, Giovenzana GB. *Org Biomol Chem*. 2014;12:6915.
- Trabocchi A, Pala N, Krimmelbein I, et al. *J Enzyme Inhib Med Chem*. 2015;30:466.
- Experimental protocol to "long lipophilic" **3c**: Methyl-11-aminoundecanoate (**13b**).¹⁶ Thionyl chloride (0.723 mL, 9.94 mmol, 2 eqs.) was added dropwise to a stirred suspension of 11-aminoundecanoic acid **12b** (1.0 g, 4.97 mmol, 1 eq.) in MeOH (5 mL) at 0 °C. After warming to rt, stirring was continued for 24 h (TLC monitoring, eluant: 9:1 CH₂Cl₂:MeOH). A 20% aqueous K₂CO₃ solution was then added until pH 9, and MeOH was removed under reduced pressure. The aqueous phase was extracted with EtOAc (3 × 15 mL), the organic phases were dried with Na₂SO₄, filtered and evaporated under reduced pressure. Aminoester **13b** (728 mg, 3.38 mmol, 68% yield) was obtained as a white solid that was used without further purification. 11-(2-Bromoacetyl-amino)-undecanoic acid methyl ester (**14b**).¹⁶ 20% Aqueous K₂CO₃ (3.6 mL, 0.872 g, 6.68 mmol, 4 eqs.) and 2-bromoacetyl bromide (0.375 mL, 4.32 mmol, 2.6 eqs.) were sequentially added dropwise to a solution of aminoester **13b** (350 mg, 1.67 mmol, 1 eq.) in CH₂Cl₂ (17 mL). The reaction mixture was vigorously stirred at rt for 3 h (TLC monitoring, eluant: 9:1 CH₂Cl₂:MeOH). The two phases were then separated and the organic phase was washed with H₂O (3 × 20 mL) and with brine (20 mL). The organic layer was dried with Na₂SO₄, filtered and the solvent was removed under reduced pressure, yielding bromoester **14b** (384 mg, 1.14 mmol, 68% yield) as a light brown oil that was used without further purification. 11-[2-(N,N-bispyridinylmethyl)aminoacetyl-amino]-undecanoic acid methyl ester (**15b**). A solution of bromoester **14b** (384 mg, 1.14 mmol, 1.1 eqs.) in dry MeCN (1.0 mL) was added to a stirred suspension of DPA **7** (0.20 mL, 1.04 mmol, 1 eq.) and NaHCO₃ (110 mg, 1.25 mmol, 1.2 eqs.) in dry MeCN (1.1 mL) at rt under nitrogen. The reaction mixture was heated at 85 °C for 2 h (TLC monitoring, eluant: 9:1 CH₂Cl₂:MeOH). The reaction mixture was then filtered and the solvent removed under reduced pressure. The crude solid (480 mg) was purified by flash chromatography (eluant: 95:5 CH₂Cl₂:MeOH), yielding pure DPA-linker ester construct **15b** (240 mg, 0.53 mmol, 51% yield) as a yellow oil. 11-[2-(N,N-bispyridinylmethyl)aminoacetyl-amino]-undecanoic acid (**11b**). 1.0 M aqueous LiOH-H₂O (0.41 mL, 0.41 mmol, 1.85 eqs.) was added to a solution of DPA-linker ester construct **15b** (100 mg, 0.22 mmol, 1 eq.) in THF (0.55 mL). The reaction mixture was stirred at rt for 39 h (TLC monitoring, eluant: 9:1 CH₂Cl₂:MeOH). THF was then removed under vacuum, and 1 M aqueous HCl was added until pH = 7. The mixture was then diluted with water (2.5 mL) and extracted with CH₂Cl₂ (3 × 2.5 mL). The collected organic phases were washed with brine (7 mL) and dried with Na₂SO₄. After solvent removal, DPA-linker acid construct **11b** (87 mg, 0.20 mmol, 89% yield) was obtained as a red oil that was used without further purification. N³-Boc protected "long lipophilic" DAC **3c** (**10c**). Dry TEA (0.14 mL, 1.02 mmol, 10 eqs.) was added to a stirred solution of DPA-linker acid construct **11b** (87 mg, 0.20 mmol, 1.95 eqs.), EDC-HCl (37 mg, 0.2 mmol, 1.95 eqs.) and HOBt (26 mg, 0.2 mmol, 1.95 eqs.) in dry CH₂Cl₂ (2.1 mL) under nitrogen. After 20 min, a solution of amine **4** (66 mg, 0.102 mmol, 1 eq.) in dry CH₂Cl₂ (3.0 mL) was added. The reaction mixture was stirred at rt for 22 h (TLC monitoring, eluant: 9:1 CH₂Cl₂:MeOH). The reaction was quenched with saturated aqueous NH₄Cl (25 mL). The organic phase was washed with saturated aqueous NH₄Cl (25 mL), saturated aqueous NaHCO₃ (25 mL) and brine (30 mL). The organic phase was dried with Na₂SO₄, filtered and the solvent was removed under reduced pressure. The crude product (95 mg) was purified by reverse phase flash chromatography (eluant: from 90:10 H₂O/MeCN to pure MeCN), yielding pure compound **10c** (45 mg, 0.0438 mmol, 42% yield) as a white solid. "Long lipophilic" **3c**. TFA (0.20 mL, 0.863 mmol, 20 eqs.) was added to a solution of compound **10c** (45 mg, 0.0434 mmol, 1 eq.) in CH₂Cl₂ (0.5 mL). The reaction mixture was stirred for 4 h at rt (TLC monitoring, eluant: 9:1 CH₂Cl₂:MeOH). The solvent was then removed under reduced pressure, repeatedly stripping the residue with toluene aliquots. The residue was then dried under vacuum yielding 0.043 g of crude solid, that was purified by reverse phase HPLC (eluant: 90:10 H₂O/MeCN to 20:80 H₂O/MeCN). Pure "long lipophilic" **3c** was obtained as a white solid (40 mg, 0.029 mmol, 67% yield).
- Zhang B, Nikolovska-Coleska Z, Zhang Y, et al. *J Med Chem*. 2008;51:7352.